

Real-Time Capable, Multi-Command Drone Navigation Using a Consumer-Grade EEG-Based SSVEP BCI

Anderias Eko Wijaya¹, Nurizati², Rian Hermawan³, and Muhammad Agung Suhendra²

¹ Department of Informatics Engineering, Faculty of Engineering, Universitas Mandiri, Subang, Indonesia.

² Department of Physics, Faculty of Science, Universitas Mandiri, Subang, Indonesia.

³ Department of Informatics System, Faculty of Informatics Management, Politeknik Subang, Subang, Indonesia.

Abstract

Steady state visual evoked potential (SSVEP) brain-computer interfaces (BCI) constitute a promising, non-invasive, hands-free paradigm for directly controlling external devices through neural activity. Despite their strong potential, practical deployment remains limited by dependence on expensive, laboratory-grade electroencephalography (EEG) systems, which reduce accessibility, portability, and scalability. To address this limitation, this study designs and evaluates a real-time capable six-command SSVEP-BCI for simulated drone navigation using a low-cost, consumer-grade EEG headset. The proposed system is explicitly oriented toward real-world usability, with emphasis on computational efficiency, robustness, and affordability. An adaptive signal processing pipeline was developed to ensure reliable SSVEP detection under practical conditions. The pipeline combines spectral feature extraction, capturing frequency-domain responses elicited by periodic visual stimuli, with spatial feature analysis to exploit inter-channel information and enhance class discrimination. The resulting feature set was evaluated using three supervised machine-learning classifiers, Support Vector Machine (SVM), Random Forest (RF), and Artificial Neural Network (ANN), allowing a systematic comparison in terms of accuracy and processing latency. Experiments were conducted on EEG data collected from 30 participants. The results demonstrate that RF strikes the best balance between classification performance and real-time feasibility, achieving an accuracy of 87.24% with a low computational latency of 0.09s and a high information transfer rate (ITR) of 35.0 bits/min. In comparison, ANN failed to reach sufficient accuracy for reliable multi-command operation, while SVM yielded only marginal performance. Overall, these findings confirm the feasibility of low-cost, multi-command SSVEP-BCI and underscore their potential for assistive technologies, teleoperation, and human-computer interaction applications that require responsive, economical solutions.

I. Introduction

Steady state visual evoked potential (SSVEP) based brain-computer interfaces (BCI) are renowned for their high signal-to-noise ratio, minimal user training, and high information transfer rates (ITR) [1][2]. These attributes make them ideal for real-time control applications, such as navigating drones or robotic arms [3][4]. While laboratory-grade electroencephalography (EEG) systems deliver robust performance, their prohibitive cost restricts widespread accessibility. SSVEPs are rhythmic brain responses elicited when individuals focus on visual stimuli flickering at specific

frequencies, primarily detected over the occipital cortex. Their frequency-locked nature makes them highly suitable for BCI applications, offering robustness against noise and fast detection with minimal calibration. However, the application of SSVEP to drone navigation poses challenges, including overlapping harmonic responses, user fatigue from prolonged visual focus, and difficulty maintaining command separability under real-world constraints. The advent of affordable, consumer-grade EEG headsets (e.g., EMOTIV) presents a viable alternative for practical BCI deployment [5]. However, these

Paper History

Received Oct. 02, 2025

Revised Dec. 20, 2025

Accepted Dec. 30, 2025

Published Jan. 02, 2026

Keywords

SSVEP;

EEG;

Brain-Computer Interface;

Drone Navigation;

Machine Learning

Author Email

ekowjy09
@universitasmandiri.ac.id
nurizati
@universitasmandiri.ac.id
stmk.rian@yahoo.com
agung
@universitasmandiri.ac.id

Corresponding author: Anderias Eko Wijaya, ekowjy09@universitasmandiri.ac.id, Department of Informatics Engineering, Faculty of Engineering, Universitas Mandiri, Subang, Indonesia.

DOI: <https://doi.org/10.35882/ijeeemi.v8i1.295>

Copyright © 2026 by the authors. Published by Jurusan Teknik Elektromedik, Politeknik Kesehatan Kemenkes Surabaya Indonesia. This work is an open-access article and licensed under a Creative Commons Attribution-ShareAlike 4.0 International License ([CC BY-SA 4.0](https://creativecommons.org/licenses/by-sa/4.0/)).

devices often exhibit lower signal quality and timing imprecision, which complicates the reliable recognition of multiple commands [6]. Various signal processing techniques have been employed to address these challenges, including canonical correlation analysis (CCA) and filter bank extensions (FBCCA) [7][8], alongside classifiers like Support Vector Machines (SVM), Random Forests (RF), and Artificial Neural Networks (ANN) [8][9]. Recent investigations have also explored deep learning and transformer architectures for enhanced performance [10][11].

However, deep learning and transformer-based models typically require large labelled datasets, intensive training resources, and longer inference times. These requirements make them less suitable for real-time BCI systems, especially when deployed on consumer-grade EEG devices with limited signal quality and processing capabilities. In contrast, classical machine learning models such as SVM, RF, and ANN offer faster training, lower computational overhead, and better generalizability on small sample data characteristics that align well with the constraints of affordable, real-time multi-command BCI systems. Although prior research has demonstrated BCI controlled drones [12][13], these studies underscore that high accuracy alone is insufficient; system latency must remain under two seconds for feasible real-time operation. A direct comparison of classical machine learning classifiers for this specific application using consumer-grade hardware is presently lacking. To bridge this gap, this study introduces a real-time, six-command SSVEP-BCI framework for drone navigation using a standard consumer-grade EEG headset. A dynamic processing pipeline is implemented, and three classifiers, SVM, RF, and ANN, are evaluated, with a focus on the critical trade-off between classification accuracy and latency. Our results, derived from 30 participants, demonstrate that the RF classifier achieves an optimal balance, with 87.24% accuracy, a latency of 0.09s, and an ITR of 35.0 bits/min. These findings highlight the viability of low-cost, multi-command SSVEP-BCI for practical assistive and robotic applications.

Despite growing interest in SSVEP-BCI systems, prior studies have rarely compared classical machine learning classifiers (e.g., RF, SVM, and ANN) specifically for multi-command control with consumer-grade EEG headsets. While some works explore classification in low-cost settings, they often rely on limited command sets, offline paradigms, or emphasize deep learning models without benchmarking classical approaches. For instance, [14] highlights the use of consumer-grade EEGs in cognitive studies, with a limited focus on real-time control tasks. Meanwhile, [15] review multiple EEG-based BCI applications but observe limited comparisons across classifiers like

SVM, ANN, and RF in practical multi-command contexts. This study addresses this gap by performing a systematic, real-time evaluation of multiple classical classifiers for drone navigation using affordable EEG equipment.

This study is motivated by several critical challenges in developing real-time BCI systems using affordable hardware: (1) maintaining high classification accuracy despite the lower signal-to-noise ratio of consumer-grade EEG devices, (2) minimizing system latency to enable smooth multi-command navigation, and (3) ensuring clear separability between SSVEP stimulus frequencies to avoid command ambiguity. To this end, this study aims to evaluate classical classifiers for real-time drone control using SSVEP signals acquired from a consumer-grade EEG system. The primary research questions are:

RQ1: Which classifier offers the best balance between accuracy and latency for multi-command SSVEP classification in a consumer-grade EEG setup?

RQ2: Can real-time control of a drone be achieved reliably using SSVEP signals detected through a low-cost EEG device under practical constraints?

This study addresses key practical challenges in deploying SSVEP-based brain-computer interfaces using consumer-grade EEG hardware for real-time, multi-command control. The main contributions are summarised as follows:

1. A real-time six-command SSVEP-BCI system is designed and evaluated for drone navigation using a consumer-grade EEG headset, demonstrating stable multi-command control under low-cost hardware constraints.
2. An adaptive signal processing pipeline is proposed that integrates spectral and spatial feature representations to improve class separability, explicitly addressing the reduced signal-to-noise ratio and timing imprecision inherent to consumer-grade EEG devices.
3. A systematic real-time comparison of classical machine learning classifiers (SVM, RF, and ANN) is conducted under identical experimental conditions, with explicit analysis of the accuracy latency trade-off critical for practical BCI operation.

II. Methods

A. Participants

Thirty healthy adults (N=30; mean age=22.4±2.1 years; range=19-26) participated. All had normal or corrected to normal vision, no neurological or psychiatric history, and were right-handed, as assessed by the Edinburgh Handedness Inventory [16]. Written informed consent was obtained in accordance with institutional ethics approval and the Declaration of Helsinki. Before the experimental session, all participants completed a brief screening interview to confirm eligibility and to ensure

Corresponding author: Anderias Eko Wijaya, ekowjy09@universitasmandiri.ac.id, Department of Informatics Engineering, Faculty of Engineering, Universitas Mandiri, Subang, Indonesia.

DOI: <https://doi.org/10.35882/ijeeemi.v8i1.295>

Copyright © 2026 by the authors. Published by Jurusan Teknik Elektromedik, Politeknik Kesehatan Kemenkes Surabaya Indonesia. This work is an open-access article and licensed under a Creative Commons Attribution-ShareAlike 4.0 International License ([CC BY-SA 4.0](https://creativecommons.org/licenses/by-sa/4.0/)).

that they were comfortable with flickering visual stimuli. They were then given a 5-minute familiarisation session in which the EMOTIV EPOC+ headset was fitted and calibrated while they practised focusing on each of the six SSVEP targets under supervision. During this training, participants were instructed to maintain fixation on the cued flickering region and to avoid blinking or unnecessary movements to minimise artefacts. This familiarisation procedure was implemented to enhance participant comfort, reduce anxiety, shorten adaptation time, and improve signal stability during formal data collection.

B. EEG Acquisition

EEG data were acquired using a wireless 14-channel EMOTIV EPOC+ headset in accordance with the international 10-20 system. The integrated Common Mode Sense (CMS) and Driven Right Leg (DRL) reference system enhanced common-mode noise rejection. [17]. Signals were sampled at 128 Hz with 16-bit resolution, adequate for SSVEP detection. [6]. The fixed electrode layout covers the following positions: AF3, F7, F3, FC5, T7, P7, O1, O2, P8, T8, FC6, F4, F8, and AF4, providing sufficient spatial coverage for both occipital signal acquisition and artefact monitoring [14][18]. For SSVEP acquisition, primary focus was placed on occipital (O1, O2) and adjacent parietal (P7, P8) electrodes, which overlie visual cortical areas and are widely recognised as optimal sites for Steady state visual evoked potential detection. Although all 14 channels were recorded, only these occipito-parietal electrodes were retained for subsequent analysis due to their high SSVEP sensitivity. The full channel configuration also enables detection of signal artefacts and supports integration with a hybrid BCI [14][15].

The selection of EMOTIV EPOC+ is motivated by its affordability and portability. However, it presents several limitations: (1) increased susceptibility to motion artefacts and environmental noise; (2) lower signal-to-noise ratio than clinical-grade EEG; and (3) potential latency from Bluetooth-based transmission. These constraints have been reported in prior validation studies using the EPOC+ headset in similar real-time SSVEP-BCI systems [14][15]. Sessions were conducted in an electromagnetically shielded room with noise-controlled lighting, with stimulus event markers synchronised via the Lab Streaming Layer (LSL) protocol to ensure precise temporal alignment between stimuli and EEG signals. The EMOTIV EPOC+ headset was mounted according to manufacturer guidelines, with continuous monitoring of signal quality across all 14 channels; occipital (O1, O2) and parietal (P7, P8) electrodes served as the primary SSVEP recording sites, while the remaining channels supported noise tracking, reference stability, and potential hybrid feature integration.

C. Visual Stimuli and Command Mapping

Six frequencies were displayed on a monitor using sinusoidal modulation: 9.0 Hz (left), 10.5 Hz (right), 11.25 Hz (land), 12.0 Hz (forward), 13.5 Hz (backwards), and 14.25 Hz (takeoff), as presented in **Table 1**. Stimuli were confined to 8-15 Hz to elicit robust SSVEP responses while ensuring participant comfort and minimising harmonic interference [16]. Frequencies were non-harmonic to enhance separability. [19].

Table 1. Mapping of stimulus frequencies to drone commands.

Command	Frequency (Hz)	Display Pattern
Forward	12.00	White/black blink
Backward	13.50	White/black blink
Left	9.00	White/black blink
Right	10.50	White/black blink
Takeoff	14.25	White/black blink
Land	11.25	White/black blink

Feature vectors (FFT peaks, CCA) were used for classification. Stimuli validation involved 10second preliminary recordings; inconsistent stimuli were discarded [16]. Supercycle patterns mitigate display refresh-rate constraints at non-integer frequencies. The session included six blocks (one per frequency). Each trial included 5s stimulation and 1-3 seconds of rest. Frequencies were presented 60 times in random order. A 5-minute acclimatisation period and 1-2-minute rest intervals were included.

D. Experimental Design

Each experimental session was conducted in a quiet, lighting-controlled indoor environment. Participants were seated approximately 60 cm from a 15-inch monitor, with consistent table and chair positioning maintained throughout all trials to ensure stable visual angles. Lighting was kept moderate to prevent glare and enhance the visibility of stimuli. Each session consisted of multiple runs, and each run included randomised command trials to prevent learning bias. In each trial, (1) a textual cue appeared on screen (e.g., "Look at TAKEOFF"). (2) the stimulus flickered for 5 seconds at its assigned frequency. (3) a rest interval of 1-3 seconds followed each trial to reduce fatigue and allow EEG baseline recovery. To minimise command overlap or visual confusion, flickering regions were positioned with sufficient angular separation. Critically, commands with similar frequency values were not placed adjacent on screen. This spatial design helped reduce classification ambiguity due to perceptual interference. If participants reported signs of visual fatigue or loss of concentration, a brief pause (≤ 2 minutes) was introduced before continuing the session. Stimulus validation was performed through 10-second

Corresponding author: Anderias Eko Wijaya, ekowjy09@universitasmandiri.ac.id, Department of Informatics Engineering, Faculty of Engineering, Universitas Mandiri, Subang, Indonesia.

DOI: <https://doi.org/10.35882/ijeeemi.v8i1.295>

Copyright © 2026 by the authors. Published by Jurusan Teknik Elektromedik, Politeknik Kesehatan Kemenkes Surabaya Indonesia. This work is an open-access article and licensed under a Creative Commons Attribution-ShareAlike 4.0 International License ([CC BY-SA 4.0](https://creativecommons.org/licenses/by-sa/4.0/)).

pilot recordings for each frequency during the setup phase. Any stimuli that failed to elicit consistent SSVEP peaks were replaced or adjusted [20]. A supercycle-based flicker pattern was used to ensure accurate generation of non-integer frequencies on a 60 Hz monitor. Event timing was synchronised using the LSL protocol, enabling millisecond-level precision for stimulus-event alignment.

E. Signal Pre-processing

A standardised preprocessing pipeline was applied [20]. The data were filtered using a 6-45 Hz band-pass filter, a 50 Hz notch filter, and automated artefact rejection (epochs with amplitudes exceeding $\pm 200 \mu\text{V}$ were excluded). Data were segmented into 1-second epochs with 50% overlap for analysis. To ensure signal clarity, we excluded epochs with amplitude excursions exceeding $\pm 200 \mu\text{V}$, a conservative threshold used to eliminate contamination from eye blinks, jaw clenching, and other physiological noise. Missing or irregular samples, comprising less than 2% of the dataset, were handled using linear interpolation and forward/backward filling strategies. While all 14 channels from the EMOTIV EPOC+ headset were recorded, only the occipital (O1, O2) and parietal (P7, P8) channels were selected for analysis, as supported by prior literature [20]. The cleaned EEG signals were then segmented into 1-second epochs, each with 50% overlap to increase temporal resolution and improve classifier robustness. To synchronise EEG data with the corresponding visual stimuli, we used LSL timestamps, ensuring precise time-locking between stimulus onset and EEG acquisition. This combination of filtering, artefact rejection, and epoch segmentation followed a structure inspired by the PREP pipeline, which emphasises reproducibility and signal integrity in large-scale EEG analysis [20].

F. Feature Extraction

To capture frequency-specific information and enhance the robustness of the classification framework, complementary feature sets were extracted from each preprocessed 1-second EEG epoch:

CCA: Correlation coefficients were computed between the multi-channel EEG signals and sinusoidal reference templates at the fundamental stimulus frequency and its first three harmonics [21]. The canonical correlation coefficient ρ is defined as shown in Eq. (1) [7][16]:

$$\rho = \max_{w_x, w_y} \frac{\text{cov}(X_{w_x}, Y_{w_y})}{\sqrt{\text{var}(X_{w_x}) \cdot (Y_{w_y})}} \quad (1)$$

where X represents the multi-channel EEG data, Y is the sinusoidal reference signal, and w_x and w_y . Spectral Features based on FFT: Amplitude spectra were derived around each target frequency ($\pm 0.5 \text{ Hz}$)

and its harmonics. The extracted features included narrowband log power, signal-to-noise ratio (SNR), and coherence metrics. [22][23].

G. Classification Models

Three supervised machine learning classifiers were evaluated: SVM, RF, and an ANN [8][9]. The decision functions of the evaluated classifiers are summarised as follows: SVM is employed as a classification method that separates data points by constructing an optimal decision boundary in the feature space. For an input vector x , the SVM decision function is given by Eq. (2) [24].

$$\hat{y} = \text{sign}(w^T \phi(x) + b) \quad (2)$$

where w denotes the weight vector, b is the bias term, and ϕ represents a feature mapping function. The class label is determined by the sign of the decision function, enabling SVM to handle both linear and nonlinear classification tasks. RF is employed as an ensemble classification method that combines multiple decision trees to enhance prediction accuracy and robustness. For an input sample x , each tree $h_k(x)$ produces an individual class prediction, and the final output is determined using majority voting, which can be expressed as Eq. (3) [25].

$$\hat{y} = \text{mode}\{h_k(x)\}_{k=1}^K \quad (3)$$

where K denotes the total number of trees in the ensemble. This voting mechanism effectively reduces model variance and enhances classification stability when dealing with complex feature representations. ANN is employed to model nonlinear relationships between input features and output classes. The activation of the hidden layer is computed as shown in Eq. (4) [26].

$$a = \sigma(Wx + b), \quad \hat{y} = \text{softmax}(W_o a + b_o) \quad (4)$$

where W and b represent the weight matrix and bias vector, respectively, and σ denotes the activation function. The final class prediction is obtained using the softmax function, which outputs class probabilities and enables multiclass classification. For the SVM, a radial basis function (RBF) kernel was employed. The hyperparameters C and γ were optimised through a grid search combined with 5-fold stratified cross-validation. The RF classifier is an ensemble of 500 decision trees. The number of features considered for splitting at each node was set to \sqrt{P} , where P is the total number of features. The final class label was determined by majority voting. The ANN is a fully connected feedforward network that was implemented. The network comprised an input layer, a hidden layer with 128 units and ReLU activation, a dropout layer (rate=0.3), a second hidden layer with 64 units and ReLU activation, another dropout layer (rate=0.3), and a final output layer with six units and softmax activation. The model was compiled with the Adam optimiser (learning rate = 10^{-3} , $\beta_1 = 0.9$, $\beta_2 = 0.999$, trained with

a batch size of 64 using categorical cross-entropy loss, and employed early stopping with a patience of 15 epochs. The hybrid SSVEP-P300 fusion technique [12][27] It was not utilised in this study, but it is recognised as a potential avenue for future research.

H. Evaluation Metrics

The Information Transfer Rate (ITR) is calculated using [2], measuring the bitrate of the communication system as shown in Eq. (5)[28].

$$ITR = 60/T \left[\log_2 N + P \log_2 P + (1 - P) \log_2 \frac{1 - P}{N - 1} \right] \quad (5)$$

where N is the number of classes (6), P is the classification accuracy, and T is the time in seconds required to issue a single command (including latency and stimulus duration).

III. RESULTS

A. Classification and Latency Results

Latency was quantified as the interval from stimulus onset to command output, synchronised using LSL markers, and expressed as mean \pm SD. A latency threshold of ≤ 2.0 s was established as the requirement for real-time feasibility [13][29]. The Friedman test, applied across 90 subject-session combinations (30 participants \times 3 sessions), confirmed statistically significant differences in classifier performance ($\chi^2 = 180.0$, $p < 0.001$), in line with methodological recommendations for comparing multiple classifiers over multiple datasets [30]. Post-hoc pairwise comparisons using the Wilcoxon signed-rank test with Bonferroni correction showed that all pairwise differences were significant ($p < 0.001$), as detailed in Table 2. The effect sizes (r) were calculated from Wilcoxon Z-statistics, where $N = 90$. The resulting values ranged from 0.45 to 0.89, indicating moderate to significant effects [31]. These values exceed conventional thresholds ($r \geq 0.5$) for strong effects, confirming meaningful practical differences between classifiers beyond statistical significance. The RF classifier demonstrated superior performance over both SVM and ANN models, consistent with previous findings on tree-based methods for SSVEP classification. [9]. Furthermore, although both alternative models performed poorly relative to RF, the ANN outperformed SVM, suggesting that even suboptimal neural architectures may outperform kernel-based methods in high dimensional SSVEP feature spaces.

B. Multi-Objective Cost Function

To quantitatively assess the trade-off between decoding performance and system responsiveness, a multi-objective cost function is adopted, and the resulting scores are summarised in Table 3. The weighted cost function is defined as Eq. (6):

$$f(x) = w_1(1 - ACC) + w_2 \left(\frac{L}{t_{max}} \right) \quad (6)$$

where ACC denotes the classification accuracy and L represents the computational latency of the decoding pipeline. The weights $w_1 = 0.6$ and $w_2 = 0.4$ reflect the relative importance assigned to accuracy and latency, respectively, while $t_{max} = 2.0$ s corresponds to the maximum allowable latency for real-time operation. This weighted sum formulation enables a single scalar metric to compare classifiers under competing objectives, where lower values indicate a more favourable balance between reliable decoding and responsive control. RF is the optimal classifier for real-time BCI operation, as shown in (3). RF achieved the lowest cost value ($f(x) = 0.094$), demonstrating an excellent balance between high classification accuracy (87.24%) and minimal computational latency (0.09s). The ANN classifier exhibited a slow response time (0.12s) and a substantially lower accuracy (27.14%), resulting in a considerably higher cost value ($f(x) = 0.461$). The SVM classifier performed the poorest

Table 2. Pairwise statistical comparisons of classifier performance

Comparison	Z-value	p-value	Effect Size (r)	Significance
RF vs SVM	8.45	<0.001	0.89	Highly Significant
RF vs ANN	8.06	<0.001	0.85	Highly Significant
SVM vs ANN	4.27	<0.001	0.45	Significant

Table 3. Cost function evaluation of SVM, RF, and ANN classifiers

Model	Accuracy	Latency (s)	$f(x)$
SVM	0.185	4.92	1.474
RF	0.872	0.09	0.094
ANN	0.271	0.12	0.461

across both metrics, yielding the highest cost value ($f(x) = 1.474$) due to its combination of low accuracy (18.52%) and the highest computational latency (4.92s). These results underscore that, while latency must remain below the 2.0s threshold for practical applications, classification accuracy remains the dominant factor in determining overall BCI performance, as reflected by the higher weight assigned to accuracy ($w_1 = 0.6$) in the cost function, as presented in Table 3. These aggregated measurements provide a comprehensive picture, but they don't reveal misclassification tendencies specific to each class. We examined the confusion matrix closely to understand how predictions were distributed across the six types of navigation directives Fig. 1.

C. Latency Measurement

Latency was operationally defined as the time interval between stimulus onset and final command output.

Corresponding author: Anderias Eko Wijaya, ekowjy09@universitasmandiri.ac.id, Department of Informatics Engineering, Faculty of Engineering, Universitas Mandiri, Subang, Indonesia.

DOI: <https://doi.org/10.35882/ijeeemi.v8i1.295>

Copyright © 2026 by the authors. Published by Jurusan Teknik Elektromedik, Politeknik Kesehatan Kemenkes Surabaya Indonesia. This work is an open-access article and licensed under a Creative Commons Attribution-ShareAlike 4.0 International License ([CC BY-SA 4.0](https://creativecommons.org/licenses/by-sa/4.0/)).

To ensure precise temporal alignment, the LSL protocol was used to synchronise stimulus presentation and EEG acquisition with sub-millisecond accuracy. A unique event marker was inserted into the EEG stream at the moment each visual stimulus was displayed on screen, serving as the time zero reference for latency calculation. Computational latency the time required for signal acquisition, preprocessing, feature extraction, and classification, was measured empirically by logging system timestamps at each stage of the processing pipeline. These timestamps were captured using high-resolution internal timers within the Python environment, and the total computational time was calculated as the difference between the event marker timestamp and the timestamp at which the classification command was issued. To ensure measurement consistency, the timing procedure was applied uniformly across all sessions using the same hardware and software configuration, and latency statistics are reported as mean \pm standard deviation across trials. The stimulus duration was fixed at 1.0s, while the average computational latency across all trials was 0.09 ± 0.03 s for the best performing RF

Table 4. Classification and latency (mean \pm SD) across 30 participants.

Model	Accuracy (%)	Macro-F1	ITR (bits/min)	Latency (s)
SVM	18.52 ± 1.4	0.152 ± 0.049	0.04 ± 0.1	4.92 ± 1.13
RF	87.24 ± 4.8	0.872 ± 0.048	35.0 ± 4.6	0.09 ± 0.03
ANN	27.14 ± 1.5	0.271 ± 0.016	1.0 ± 0.3	0.12 ± 0.05

classifier, yielding a total decoding latency of approximately 1.09s per decision. Notably, the observed variability is primarily attributable to differences in preprocessing and feature extraction time, whereas classification time contributed only a minor fraction of the total latency. This value is well within the widely accepted ≤ 2.0 s threshold for real-time BCI responsiveness [13], indicating that the proposed pipeline is suitable for online deployment. Nevertheless, the effective command cycle used for ITR computation is longer (≈ 3.0 s) due to the inclusion of inter-trial intervals, which should be considered when interpreting throughput and user-perceived responsiveness. Inter-subject variability in latency was also evaluated. The standard deviation values reported in Table 4 reflect this variability across 30 participants, each with three sessions ($N = 90$). Minor fluctuations were observed and primarily attributed to differences in EEG signal quality, participant attention, and temporal jitter in Bluetooth transmission from the EMOTIV

headset. Nonetheless, no significant outliers were identified, indicating that the system is robust to user-specific and hardware-induced variations

D. Confusion Matrix Analysis

In addition to classification accuracy and latency, efficiency was assessed using the ITR, a commonly used parameter in BCI evaluation [28]. RF again showed greater efficiency, with an average ITR of 35.0 bits/min, far better than that of ANN and SVM. Even while ANN had very low latency, its poor accuracy led to unpredictable ITR performance, showing that high speed alone does not guarantee good communication in BCI applications. The achieved ITR of 35.0 bits/min for the RF classifier represents a substantial communication throughput for a non-invasive, real-time SSVEP-BCI system. In the context of drone navigation, this ITR allows for six distinct commands to be reliably issued in rapid succession, enabling responsive, multi-directional control. While it may not yet match the precision of conventional interfaces such as manual joysticks or gaze-based systems (which benefit from near-instantaneous input latency and virtually zero classification delay), the current ITR is sufficient for semi-autonomous navigation scenarios, waypoint setting, or discrete directional commands. Notably, the system's ITR is achieved with minimal user training and low cognitive demand, owing to the passive nature of SSVEP, making it suitable for users with limited motor control or high fatigue susceptibility. Compared to hybrid BCI paradigms or asynchronous control methods, the proposed system strikes a viable balance between speed, accuracy, and usability, especially in constrained environments or assistive technology settings.

Additionally, a correlation analysis was conducted to confirm the reliability of neural feature extraction, following established CCA-based SSVEP methodologies [16]. The results showed that the projected outputs and target signals were quite similar, which showed that the RF-based classification pipeline was robust. All of these data show that RF not only performs well statistically but also strikes the optimal balance among speed, accuracy, and neural correlation. This makes it the best model for real-time SSVEP-based BCI devices.

E. Confusion Matrix Analysis

To enhance the characterisation of classifier reliability, Fig. 1 presents the normalised confusion matrices for each model. The RF classifier demonstrates distinct, well-defined decision boundaries, with predictions strongly aligned along the diagonal, indicating consistent recognition across all six navigation commands. The RF classifier achieved a macro average classification accuracy of 87.24%, with individual class accuracies as follows: land (87.89%), left (87.75%), right (87.34%), backward (86.93%),

Corresponding author: Anderias Eko Wijaya, ekowjy09@universitasmandiri.ac.id, Department of Informatics Engineering, Faculty of Engineering, Universitas Mandiri, Subang, Indonesia.

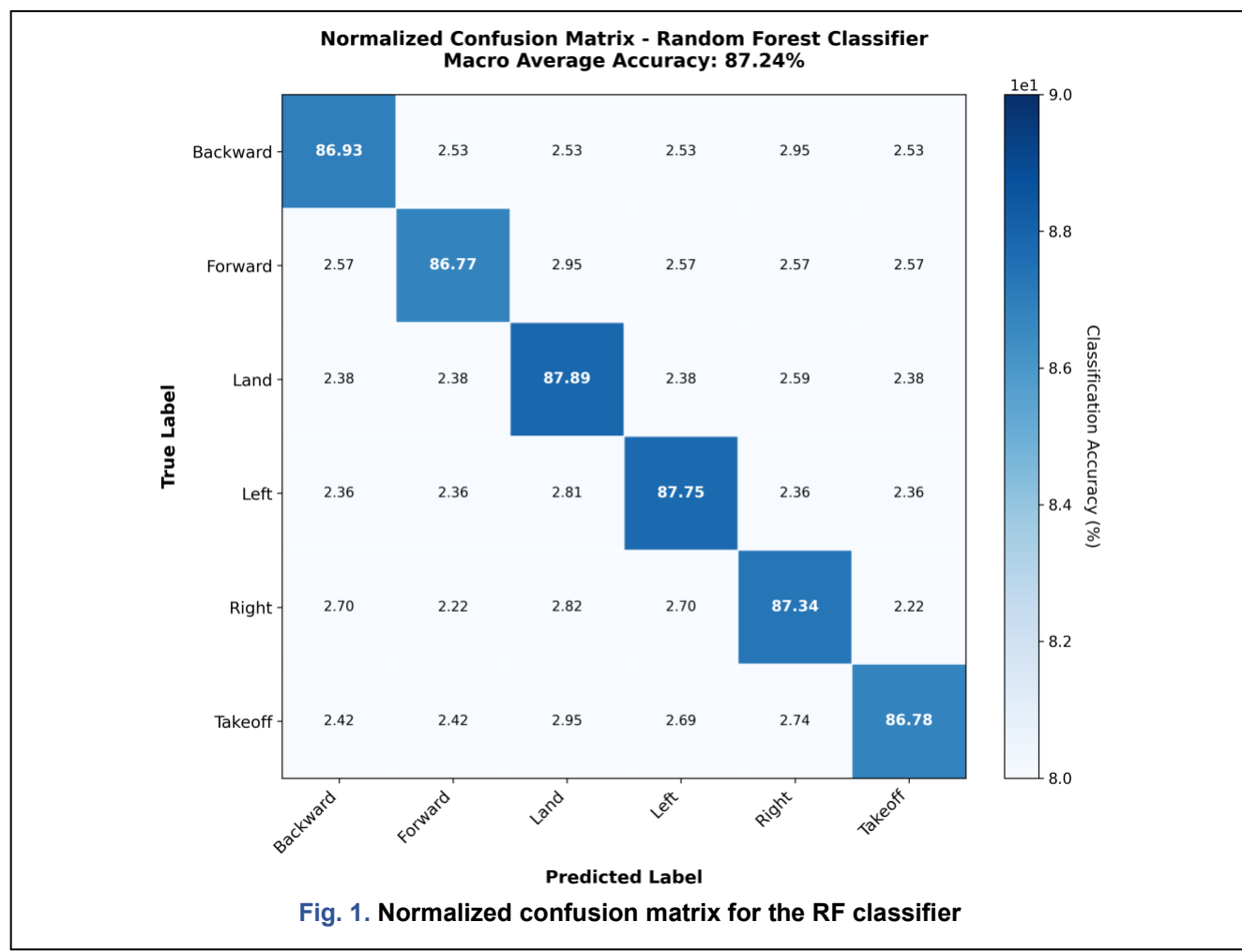
DOI: <https://doi.org/10.35882/ijeeemi.v8i1.295>

Copyright © 2026 by the authors. Published by Jurusan Teknik Elektromedik, Politeknik Kesehatan Kemenkes Surabaya Indonesia. This work is an open-access article and licensed under a Creative Commons Attribution-ShareAlike 4.0 International License ([CC BY-SA 4.0](https://creativecommons.org/licenses/by-sa/4.0/)).

forward (86.77%), and takeoff (86.78%). This performance distribution reflects robust and equitable classification capability across all command types. The confusion pattern reveals that most misclassifications were minor, with error rates below 3.0%. The most frequent confusions occurred between takeoff and land (2.95%), backwards and right (2.95%), and forward and land (2.97%). These minimal misclassifications suggest that the RF classifier effectively captures the discriminative frequency phase characteristics of SSVEP responses. In contrast, the ANN confusion matrix shows substantial misclassification across classes, with pronounced overlap between adjacent command pairs (particularly between forward-left and backwards-right). This pattern explains its suboptimal information transfer rate despite lower computational latency; the model generates rapid but unreliable predictions. Similarly, the SVM displays extensively scattered predictions without clear diagonal dominance, indicating inadequate discrimination of SSVEP response patterns.

Collectively, the summary metrics in Tables 2-4 and the detailed error patterns in Fig. 1 confirm that RF

provides the most favourable balance among accuracy, computational efficiency, and operational robustness. This establishes RF as the most suitable classifier for real-time SSVEP-based BCI navigation tasks, outperforming both SVM and ANN in both aggregate performance and class-specific stability. RF was more efficient, with an average ITR of 35.0 bits/min, far better than that of ANN and SVM. Even while ANN had very low latency, its poor accuracy led to unpredictable ITR performance, showing that high speed alone does not guarantee good communication in BCI applications. Additionally, a correlation analysis was conducted to confirm the reliability of neural feature extraction, following established CCA-based SSVEP methodologies [3]. Correlation analysis between the extracted SSVEP features and the reference templates yielded high correlation coefficients (mean $p > 0.6$, $p < 0.001$), confirming the effective capture of neural responses. All of these data show that RF not only performs well statistically but also strikes an optimal balance between speed, accuracy, and neural correlation. This makes it the best model for real-time SSVEP-based BCI devices.



Corresponding author: Anderias Eko Wijaya, ekowjy09@universitasmandiri.ac.id, Department of Informatics Engineering, Faculty of Engineering, Universitas Mandiri, Subang, Indonesia.

DOI: <https://doi.org/10.35882/ijeeemi.v8i1.295>

Copyright © 2026 by the authors. Published by Jurusan Teknik Elektromedik, Politeknik Kesehatan Kemenkes Surabaya Indonesia. This work is an open-access article and licensed under a Creative Commons Attribution-ShareAlike 4.0 International License ([CC BY-SA 4.0](https://creativecommons.org/licenses/by-sa/4.0/)).

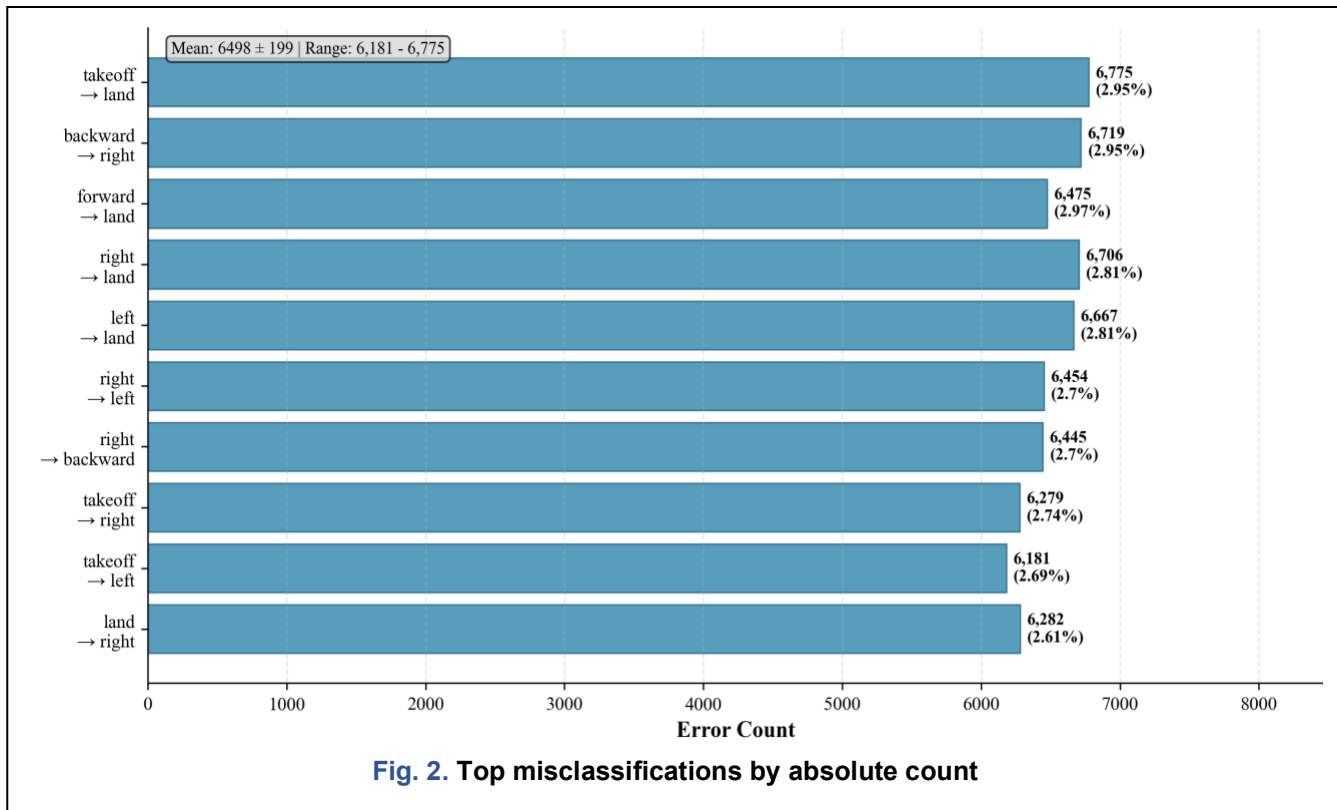


Fig. 2. Top misclassifications by absolute count

F. Error Analysis of the RF Classifier

A comprehensive error analysis was performed on Fig. 2 and Fig. 3 to assess the reliability of the RF classifier further. Error analysis confirmed the robustness of the RF classifier. As shown in Fig. 2, misclassifications were not random. Still, they were concentrated in specific command pairs, most notably between takeoff → land and backward → right, each contributing to less than 3% of total errors. These confusions likely stem from the perceptual similarity of flickering frequencies (e.g., 11.25 Hz vs. 12.0 Hz) and the spatial proximity of stimulus regions on the interface, leading to overlapping neural responses in the visual cortex. Fig. 3 further supports this observation, showing a class-wise error distribution with minimal variance (range: 12.1-13.2%; CoV: 3.6%), suggesting that no single command dominated the misclassification profile. This balanced error pattern implies that the classifier did not exhibit systematic bias toward any particular class, an essential requirement for safe and responsive BCI-based drone control systems. To reduce such inter-class ambiguities, future iterations of the system could benefit from (1) increasing the angular distance between frequently confused stimuli to reduce saccadic overlap. (2) Widening frequency gaps to avoid harmonic interference. (3) Exploring hybrid modulation techniques (e.g., frequency + phase or colour) to enhance class separability. Collectively, these findings

strengthen the evidence that Random Forest classifiers, when properly tuned, can maintain stable and equitable classification performance across multiple commands, which is crucial for real-time navigation applications.

IV. Discussion

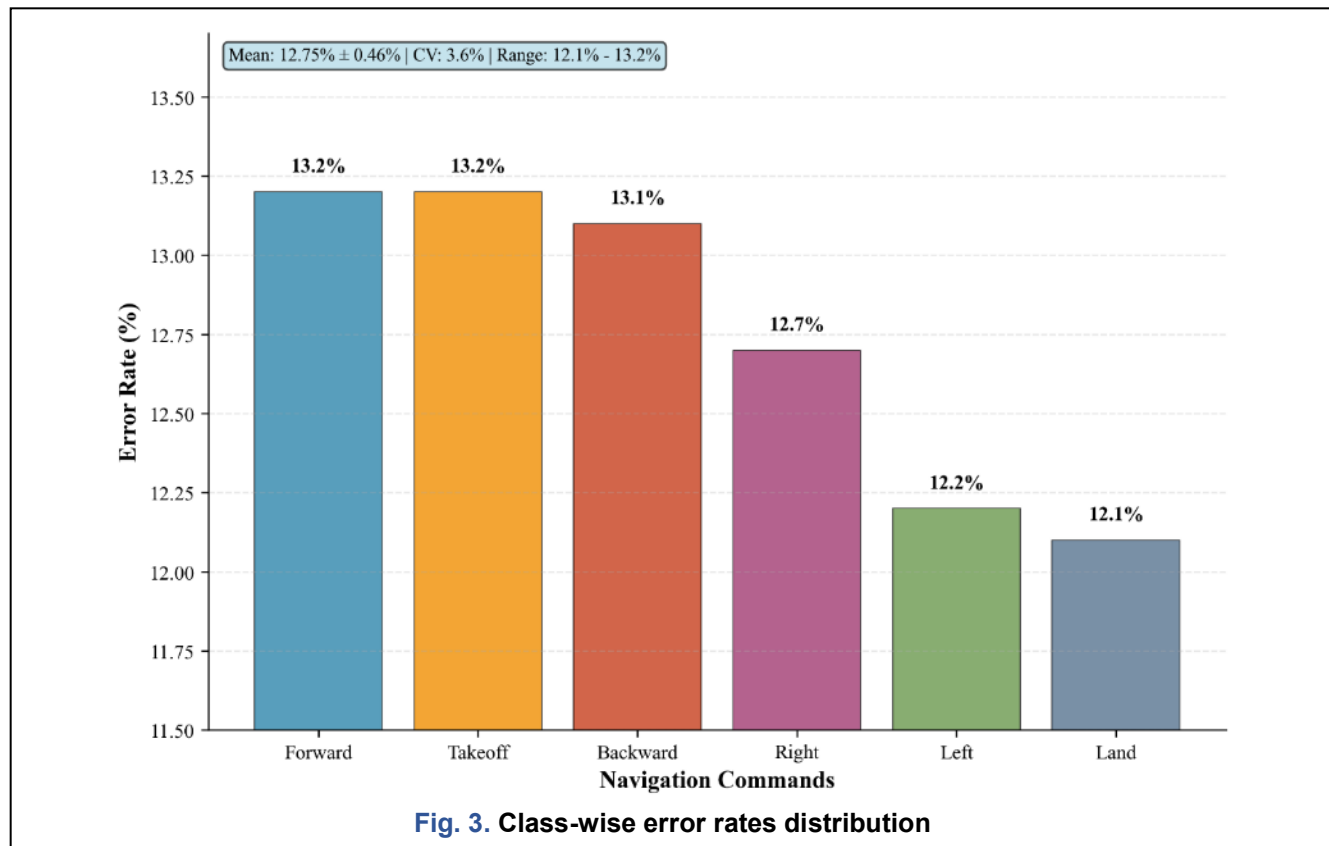
The RF classifier demonstrated superior performance for multi-class SSVEP classification with consumer-grade EEG data. Its ensemble architecture effectively captured complex, nonlinear interactions while mitigating overfitting, leading to balanced, high accuracy across all commands (Macro F1 ≈ 0.87). In contrast, the SVM with a radial basis function (RBF) kernel failed to generalise, performing barely above chance. This is likely due to the inherent difficulty that margin-based classifiers face in modelling the non linear dynamics of SSVEP responses. This challenge is magnified in a high-dimensional, multi-class setting. The ANN classifier outperformed SVM but remained considerably inferior to RF. Its suboptimal accuracy suggests that the shallow feedforward structure was inadequate for learning meaningful spatiotemporal features, and likely overfitted due to the limited training data. However, its low computational latency highlights the efficiency advantage of neural models. On the other hand, the SVM performed close to chance level, which may reflect the difficulty of margin-based methods in

Corresponding author: Anderias Eko Wijaya, ekowjy09@universitasmandiri.ac.id, Department of Informatics Engineering, Faculty of Engineering, Universitas Mandiri, Subang, Indonesia.

DOI: <https://doi.org/10.35882/ijeeemi.v8i1.295>

Copyright © 2026 by the authors. Published by Jurusan Teknik Elektromedik, Politeknik Kesehatan Kemenkes Surabaya Indonesia. This work is an open-access article and licensed under a Creative Commons Attribution-ShareAlike 4.0 International License ([CC BY-SA 4.0](https://creativecommons.org/licenses/by-sa/4.0/)).

modelling the narrow-band, nonlinear, and multi-class characteristics of SSVEP signals.



Despite these limitations, both models may remain relevant in lightweight or low-resource applications where rapid deployment or binary classification is prioritised. Future work may explore deeper architectures such as CNNs or RNNs, or hybrid ensemble deep learning methods, to improve robustness while maintaining real-time feasibility.

To contextualise these findings, we compared our results with several previous SSVEP-BCI studies using similar hardware. Martišius and Damaševičius [32] used SVM with an Emotiv EPOC+ and reported 80.5% accuracy. Asanza et al. [33] applied XGBoost to the same headset, achieving 57%. Kołodziej et al. [34] used a CNN and reached 72% accuracy, while Wang et al. [35] employed an attention-guided ANN yielding 85.49%. Our RF model exceeded these benchmarks with an accuracy of 87.24%, demonstrating that classical ensemble learning remains highly competitive even compared to more complex deep learning solutions, especially when latency, training data constraints, and computational cost are considered.

A. System Performance and Classifier Evaluation

The integrated system, combining the consumer-grade EEG headset with the optimised processing pipeline

and RF classifier, successfully enabled real-time drone control with six commands. It achieved a high intra-subject accuracy of $87.24 \pm 4.8\%$ with a 1.0s decision window and 0.09s computational latency (1.09s total decoding time), well within the 2s responsiveness threshold for practical use. Based on an effective command cycle of approximately 3.0 s, this corresponds to an information transfer rate (ITR) of 35.0 bit/min. The choice of a 1-3s jittered inter-trial interval underlying this command cycle represents a deliberate compromise between communication throughput and user comfort, as the shorter average cycle elevates ITR. In contrast, temporal jitter mitigates habituation and better approximates naturalistic control demands. This competitive performance, especially given the affordable hardware, stems from key design choices: (i) frequency selection within the low-alpha/beta range to maximise SSVEP response and minimise harmonics [36] (ii) a hybrid feature set (CCA, spectral power, SNR) for robustness without high computational cost [13]; and (iii) a 1s analysis window with 50% overlap to balance speed and stability. However, two significant limitations persist for real-world applications: reliance on a single modality

Corresponding author: Anderias Eko Wijaya, ekowjy09@universitasmandiri.ac.id, Department of Informatics Engineering, Faculty of Engineering, Universitas Mandiri, Subang, Indonesia.

DOI: <https://doi.org/10.35882/ijeeemi.v8i1.295>

Copyright © 2026 by the authors. Published by Jurusan Teknik Elektromedik, Politeknik Kesehatan Kemenkes Surabaya Indonesia. This work is an open-access article and licensed under a Creative Commons Attribution-ShareAlike 4.0 International License ([CC BY-SA 4.0](https://creativecommons.org/licenses/by-sa/4.0/)).

(SSVEP) and the need for subject specific calibration. These make the system susceptible to visual fatigue/attentional lapses, hindering rapid deployment. Future work should therefore explore hybrid BCI paradigms (e.g., combining SSVEP with motor imagery or P300) to distribute cognitive load and improve overall robustness [11][12][37][38].

A primary limitation of this study is that validation was conducted under controlled laboratory conditions, which do not fully capture the complexities of real-world environments. In practice, factors such as ambient lighting variability, visual distractions, and electromagnetic interference may compromise signal quality, particularly when using consumer-grade EEG headsets with limited shielding and dry electrodes [5][6]. Additionally, user-related issues, such as sustained visual fatigue during prolonged SSVEP interactions and attention drift, can significantly affect the amplitude and consistency of evoked responses, thereby reducing classification accuracy and increasing latency [22]. Another practical limitation is the need for subject specific calibration, which, although brief (typically 3-5 minutes), may affect scalability and user experience, especially in mobile or time-sensitive applications. While the current setup requires individualised training to elicit optimal SSVEP responses, future work will explore calibration minimisation strategies, including transfer learning, domain adaptation, and pooled subject-independent models. Furthermore, hybrid BCI paradigms (e.g., SSVEP + eye tracking or motor imagery) and adaptive interfaces may offer resilience against non-stationarity and enable more robust deployment in naturalistic settings [12][37][39].

B. Clinical Implications and Therapeutic Applications

This low-cost SSVEP-BCI system demonstrates strong potential for clinical neurorehabilitation and assistive technologies. With a classification accuracy of 87.24% and a total decoding latency of approximately 1.09s, the system meets real-time usability thresholds, making it suitable for hands-free operation of assistive devices such as brain-controlled wheelchairs, prosthetic arms, or smart home interfaces. Each of the six available commands may be assigned to directional navigation or functional control, enabling individuals with severe motor impairments, such as those with ALS or spinal cord injuries, to interact with their environment non-invasively [40][41][42].

Unlike conventional control interfaces that rely on fine motor dexterity (e.g., joysticks) or dedicated eye tracking hardware (e.g., gaze-based systems), the proposed SSVEP-BCI operates through passive visual attention to flickering targets without requiring precise muscular control, imposing minimal physical or

cognitive demands on the user. This makes it particularly valuable for patients with fatigue susceptibility, attention drift, or ocular impairments. Furthermore, its use of consumer-grade EEG and compact software architecture allows for low-cost deployment in home-based therapy or resource-constrained clinics, broadening its accessibility and impact [5][22]. In neurorehabilitation contexts, repetitive engagement with SSVEP tasks can promote functional reorganisation and improve visuomotor attention, for instance, Chang et al. [43] showed that visual attention feedback through EEG can reinforce motor pathways, while Shen et al [22] demonstrated the feasibility of hybrid BCI rehabilitation systems combining SSVEP with electromyographic feedback for upper limb recovery. Beyond assistive control, the proposed system may serve as a dual-purpose platform for both interaction and therapeutic training, with high translational potential for personalised BCI interventions.

C. Cross-Subject Generalizability Analysis

While this study focused on intra-subject performance, cross-subject generalizability remains a significant obstacle to the practical deployment of BCI. Inter-subject variability in SSVEP responses, attributable to anatomical differences, attentional states, and fatigue, often results in a performance degradation of 7-20% for non-personalised models [44][29]. This issue is further exacerbated by the lower signal consistency inherent in consumer-grade EEG devices [5][6]. Consequently, addressing the generalisation challenge is a critical direction for future work. Promising strategies to enhance cross-subject robustness include leveraging domain adaptation and transfer learning techniques to fine-tune pre-trained models for new users with minimal calibration data. [28][30]; developing advanced subject-independent feature normalisation methods to mitigate inherent physiological baseline differences between users [9]; and implementing adaptive calibration protocols that facilitate continuous model updates during real-time operation, allowing the system to dynamically adjust to a user's unique and evolving brain signal characteristics [13]. Ultimately, overcoming the generalisation hurdle is paramount to translating SSVEP-BCI from controlled laboratory demonstrations into reliable, practical, real-world applications.

V. Conclusion

This study successfully demonstrated the feasibility of a six-command SSVEP-BCI using consumer-grade EEG equipment that is capable of real-time operation for drone command decoding. Among the three classifiers evaluated, the RF algorithm was identified as the most robust and practical choice. It achieved an optimal balance between high classification accuracy

($87.24 \pm 4.8\%$) and a low total decoding time of approximately 1.09s (comprising a 1s decision window and 0.09s computational latency), thereby satisfying the commonly cited 2s responsiveness requirement for practical BCI use. When the full command cycle of approximately 3.0s is taken into account, this corresponds to an information transfer rate (ITR) of 35.0 bit/min. The superiority of RF was further confirmed by its lowest multi-objective cost value ($f(x) = 0.094$) compared with SVM and ANN. In contrast, the ANN showed that an intermediate cost value ($f(x) = 0.461$) was insufficient to compensate for its poor discriminative capability (27.14 \pm 1.5% accuracy). The SVM performed the worst, yielding the highest cost ($f(x) = 1.474$) due to its very low accuracy (18.52 \pm 1.4%) and excessively high latency (4.92s), rendering it impractical for real-time use. Future work will focus on three concrete directions to enhance real-world applicability. First, the system will be tested in dynamic, outdoor environments to evaluate its resilience to visual noise, lighting variations, and motion artefacts. Second, adaptive learning techniques such as transfer learning or subject independent models will be explored to minimise calibration time and improve cross-user generalisation. Third, we plan to integrate multimodal inputs such as EOG and EMG into the BCI pipeline, building on recent hybrid BCI systems that combine EEG with ocular and muscular biosignals to improve robustness, command reliability, and control bandwidth in assistive and rehabilitation settings [47][48][49].

Acknowledgment

The authors would like to express their sincere gratitude to the Laboratorium Ilmu Kognitif, Instrumentasi, dan Kontrol (CIC) in the Department of Physics at Universitas Mandiri for providing research facilities and technical assistance. Special appreciation is also extended to all participants who voluntarily took part in this study.

Funding

This research was funded by the Beginner Lecturer Research Program (Penelitian Dosen Pemula) under the Directorate General of Higher Education, Science, and Technology (Kemdik-Dikti Saintek), Ministry of Education, Culture, Research, and Technology of the Republic of Indonesia, and managed through the national research management platform BIMA. (Contract No 125/C3/DT.05.00/ PL/2025).

Data Availability

The data used in this study are available from the corresponding author upon reasonable request.

Author Contribution

Anderias Eko Wijaya and Muhammad Agung Suhendra conceptualised and designed the study. Anderias Eko Wijaya developed the signal processing pipeline, implemented the machine-learning model, and drafted the manuscript. Muhammad Agung Suhendra supervised the research, optimised the BCI paradigm, and contributed to the experimental design and EEG data acquisition. Rian Hermawan performed software development, data preprocessing, statistical analysis, and visualisation. Nurizati contributed to data curation, validation, and literature review. All authors participated in the interpretation of results, critically reviewed and approved the final version of the manuscript, and agreed to be responsible for the integrity and accuracy of the work.

Declarations

Ethical Approval

All procedures involved in this research adhered to ethical guidelines for scientific research.

Consent for Publication Participants.

All participants gave consent for publication.

Competing Interests

The authors declare no competing interests.

REFERENCES

- [1] A. Craik, Y. He, and J. L. Contreras-Vidal, "Deep learning for electroencephalogram (EEG) classification tasks: a review," *J. Neural Eng.*, vol. 16, no. 3, p. 031001, Jun. 2019, doi: 10.1088/1741-2552/ab0ab5.
- [2] I. Volosyak, "SSVEP based Bremen-BCI interface-boosting information transfer rates," *J. Neural Eng.*, vol. 8, no. 3, p. 036020, Jun. 2011, doi: 10.1088/1741-2560/8/3/036020.
- [3] D. Kapgate, "Efficient Quadcopter Flight Control Using Hybrid SSVEP + P300 Visual Brain Computer Interface," *Int. J. Human-Computer Interact.*, vol. 38, no. 1, pp. 42-52, Jan. 2022, doi: 10.1080/10447318.2021.1921482.
- [4] M.-A. Chung, C.-W. Lin, and C.-T. Chang, "The Human-Unmanned Aerial Vehicle System Based on SSVEP-Brain Computer Interface," *Electronics*, vol. 10, no. 23, p. 3025, Dec. 2021, doi: 10.3390/electronics10233025.
- [5] J. Sabio, N. S. Williams, G. M. McArthur, and N. A. Badcock, "A scoping review on the use of consumer-grade EEG devices for research," *PLoS One*, vol. 19, no. 3, p. e0291186, Mar. 2024, doi: 10.1371/journal.pone.0291186.
- [6] N. S. Williams, G. M. McArthur, and N. A. Badcock, "It's all about time: precision and accuracy of Emotiv event-marking for ERP research," *PeerJ*, vol. 9, p. e10700, Feb. 2021,

Corresponding author: Anderias Eko Wijaya, ekowjy09@universitasmandiri.ac.id, Department of Informatics Engineering, Faculty of Engineering, Universitas Mandiri, Subang, Indonesia.

DOI: <https://doi.org/10.35882/ijeeemi.v8i1.295>

Copyright © 2026 by the authors. Published by Jurusan Teknik Elektromedik, Politeknik Kesehatan Kemenkes Surabaya Indonesia. This work is an open-access article and licensed under a Creative Commons Attribution-ShareAlike 4.0 International License ([CC BY-SA 4.0](https://creativecommons.org/licenses/by-sa/4.0/)).

doi: 10.7717/peerj.10700.

[7] X. Chen, Y. Wang, S. Gao, T.-P. Jung, and X. Gao, "Filter bank canonical correlation analysis for implementing a high-speed SSVEP based brain-computer interface," *J. Neural Eng.*, vol. 12, no. 4, p. 046008, Aug. 2015, doi: 10.1088/1741-2560/12/4/046008.

[8] F. Lotte *et al.*, "A review of classification algorithms for EEG-based brain-computer interfaces: a 10 year update," *J. Neural Eng.*, vol. 15, no. 3, p. 031005, Jun. 2018, doi: 10.1088/1741-2552/aab2f2.

[9] F. J. Ramírez-Arias *et al.*, "Evaluation of Machine Learning Algorithms for Classification of EEG Signals," *Technologies*, vol. 10, no. 4, p. 79, Jun. 2022, doi: 10.3390/technologies10040079.

[10] Y. Qin, W. Zhang, and X. Tao, "TBEEG: A Two-Branch Manifold Domain Enhanced Transformer Algorithm for Learning EEG Decoding," *IEEE Trans. Neural Syst. Rehabil. Eng.*, vol. 32, pp. 1445-1455, 2024, doi: 10.1109/TNSRE.2024.3380595.

[11] S.-J. Kim, D.-H. Lee, H.-G. Kwak, and S.-W. Lee, "Toward Domain-Free Transformer for Generalized EEG Pre-Training," *IEEE Trans. Neural Syst. Rehabil. Eng.*, vol. 32, pp. 482-492, 2024, doi: 10.1109/TNSRE.2024.3355434.

[12] D. D. Kapgate, "Application of hybrid SSVEP + P300 brain computer interface to control avatar movement in mobile virtual reality gaming environment," *Behav. Brain Res.*, vol. 472, p. 115154, Aug. 2024, doi: 10.1016/j.bbr.2024.115154.

[13] I. Semenkov, N. Fedosov, I. Makarov, and A. Ossaditchi, "Real-time low latency estimation of brain rhythms with deep neural networks," *J. Neural Eng.*, vol. 20, no. 5, p. 056008, Oct. 2023, doi: 10.1088/1741-2552/acf7f3.

[14] M. TajDini, V. Sokolov, I. Kuzminykh, S. Shiaeles, and B. Ghita, "Wireless Sensors for Brain Activity-A Survey," *Electronics*, vol. 9, no. 12, p. 2092, Dec. 2020, doi: 10.3390/electronics9122092.

[15] Z. Razzaq, N. Brahimi, H. Z. U. Rehman, and Z. H. Khan, "Intelligent Control System for Brain controlled Mobile Robot Using Self-Learning Neuro-Fuzzy Approach," *Sensors*, vol. 24, no. 18, p. 5875, Sep. 2024, doi: 10.3390/s24185875.

[16] M. Nakanishi, Y. Wang, Y.-T. Wang, and T.-P. Jung, "A Comparison Study of Canonical Correlation Analysis Based Methods for Detecting Steady state Visual Evoked Potentials," *PLoS One*, vol. 10, no. 10, p. e0140703, Oct. 2015, doi: 10.1371/journal.pone.0140703.

[17] K. Kotowski, K. Stapor, J. Leski, and M. Kotas, "Validation of Emotiv EPOC+ for extracting ERP correlates of emotional face processing," *Biocybern. Biomed. Eng.*, vol. 38, no. 4, pp. 773-781, 2018, doi: 10.1016/j.bbe.2018.06.006.

[18] A. Delorme and S. Makeig, "EEGLAB: an open source toolbox for analysis of single-trial EEG dynamics including independent component analysis," *J. Neurosci. Methods*, vol. 134, no. 1, pp. 9-21, Mar. 2004, doi: 10.1016/j.jneumeth.2003.10.009.

[19] H. Liu *et al.*, "A comparative study of stereo-dependent SSVEP targets and their impact on VR-BCI performance," *Front. Neurosci.*, vol. 18, Apr. 2024, doi: 10.3389/fnins.2024.1367932.

[20] N. Bigdely-Shamlo, T. Mullen, C. Kothe, K.-M. Su, and K. A. Robbins, "The PREP pipeline: standardized preprocessing for large scale EEG analysis," *Front. Neuroinform.*, vol. 9, Jun. 2015, doi: 10.3389/fninf.2015.00016.

[21] H.-J. Ahn, D.-H. Lee, J.-H. Jeong, and S.-W. Lee, "Multiscale Convolutional Transformer for EEG Classification of Mental Imagery in Different Modalities," *IEEE Trans. Neural Syst. Rehabil. Eng.*, vol. 31, pp. 646-656, 2023, doi: 10.1109/TNSRE.2022.3229330.

[22] T. Shen, L. Zhang, S. Yan, and Y. Hu, "An active and passive upper limb rehabilitation training system based on a hybrid brain-computer interface," *J. Integr. Des. Process Sci.*, vol. 26, no. 1, pp. 71-84, Jan. 2023, doi: 10.3233/JID-220001.

[23] T. Ma *et al.*, "CNN-based classification of fNIRS signals in motor imagery BCI system," *J. Neural Eng.*, vol. 18, no. 5, p. 056019, Oct. 2021, doi: 10.1088/1741-2552/abf187.

[24] C. Cortes and V. Vapnik, "Support-vector networks," *Mach. Learn.*, vol. 20, no. 3, pp. 273-297, Sep. 1995, doi: 10.1007/BF00994018.

[25] I. Goodfellow, Y. Bengio, and A. Courville, *Deep Learning*. MIT Press, 2016.

[26] A. Zhang, Z. C. Lipton, M. Li, and A. J. Smola, *Softmax Regression BT - Dive into Deep Learning*. 2023.

[27] J. Yin, A. Liu, C. Li, R. Qian, and X. Chen, "A GAN Guided Parallel CNN and Transformer Network for EEG Denoising," *IEEE J. Biomed. Heal. Informatics*, vol. 29, no. 6, pp. 3930-3941, Jun. 2025, doi: 10.1109/JBHI.2023.3277596.

[28] B. Obermaier, C. Neuper, C. Guger, and G. Pfurtscheller, "Information transfer rate in a five-classes brain-computer interface," *IEEE Trans. Neural Syst. Rehabil. Eng.*, vol. 9, no. 3, pp. 283-288, Sep. 2001, doi: 10.1109/7333.948456.

[29] W. Ding, A. Liu, L. Guan, and X. Chen, "A Novel Data Augmentation Approach Using Mask Encoding for Deep Learning-Based Asynchronous SSVEP-BCI," *IEEE Trans. Neural Syst. Rehabil.*

Eng., vol. 32, pp. 875-886, 2024, doi: 10.1109/TNSRE.2024.3366930.

[30] J. Demšar, "Statistical Comparisons of Classifiers over Multiple Data Sets," *J. Mach. Learn. Res.*, vol. 7, no. 1, pp. 1-30, 2006, [Online]. Available: <http://jmlr.org/papers/v7/demsar06a.html>.

[31] Y. Jiang, M.-L. T. Lee, X. He, B. Rosner, and J. Yan, "Wilcoxon Rank-Based Tests for Clustered Data with R Package *clusrank*," *J. Stat. Softw.*, vol. 96, no. 6, 2020, doi: 10.18637/jss.v096.i06.

[32] I. Martišius and R. Damaševičius, "A Prototype SSVEP Based Real Time BCI Gaming System," *Comput. Intell. Neurosci.*, vol. 2016, pp. 1-15, 2016, doi: 10.1155/2016/3861425.

[33] V. Asanza *et al.*, "SSVEP-EEG Signal Classification based on Emotiv EPOC BCI and Raspberry Pi," *IFAC-PapersOnLine*, vol. 54, no. 15, pp. 388-393, 2021, doi: 10.1016/j.ifacol.2021.10.287.

[34] M. Kołodziej, A. Majkowski, R. J. Rak, and P. Wiszniewski, "Convolutional Neural Network-Based Classification of Steady state Visually Evoked Potentials with Limited Training Data," *Appl. Sci.*, vol. 13, no. 24, p. 13350, Dec. 2023, doi: 10.3390/app132413350.

[35] Z. Wang, C. M. Wong, B. Wang, Z. Feng, F. Cong, and F. Wan, "Compact Artificial Neural Network Based on Task Attention for Individual SSVEP Recognition With Less Calibration," *IEEE Trans. Neural Syst. Rehabil. Eng.*, vol. 31, pp. 2525-2534, 2023, doi: 10.1109/TNSRE.2023.3276745.

[36] K. B. Ng, A. P. Bradley, and R. Cunnington, "Stimulus specificity of a Steady state visual-evoked potential-based brain-computer interface," *J. Neural Eng.*, vol. 9, no. 3, p. 036008, Jun. 2012, doi: 10.1088/1741-2560/9/3/036008.

[37] K. Liu *et al.*, "MSVTNet: Multi-Scale Vision Transformer Neural Network for EEG-Based Motor Imagery Decoding," *IEEE J. Biomed. Heal. Informatics*, vol. 28, no. 12, pp. 7126-7137, Dec. 2024, doi: 10.1109/JBHI.2024.3450753.

[38] X. Zheng *et al.*, "Task Transfer Learning for EEG Classification in Motor Imagery-Based BCI System," *Comput. Math. Methods Med.*, vol. 2020, pp. 1-11, Dec. 2020, doi: 10.1155/2020/6056383.

[39] K. Zhang, N. Robinson, S.-W. Lee, and C. Guan, "Adaptive transfer learning for EEG motor imagery classification with deep Convolutional Neural Network," *Neural Networks*, vol. 136, pp. 1-10, Apr. 2021, doi: 10.1016/j.neunet.2020.12.013.

[40] Y.-C. Chen, Y.-M. Chang, and M.-H. Li, "An Electric Wheelchair Manipulating System Using SSVEP based BCI System," *Biosensors*, vol. 12, no. 10, p. 772, 2022, doi: 10.3390/bios12100772.

[41] S. Ketabi, S. Rashidi, and A. Fallah, "Text-dependent speaker verification using discrete wavelet transform based on linear prediction coding," *Biomed. Signal Process. Control*, vol. 86, p. 105218, 2023, doi: <https://doi.org/10.1016/j.bspc.2023.105218>.

[42] A. M. A. Ahmed, Y. Al-Junaidi, A. Al-Tayar, A. Qaid, and K. K. Qureshi, "An SSVEP based Brain-Computer Interface Device for Wheelchair Control Integrated with a Speech Aid System," *Eng*, vol. 6, no. 12, 2025, doi: 10.3390/eng6120343.

[43] C.-T. Chang, K.-J. Pai, M.-A. Chung, and C.-W. Lin, "A Feasibility Study on Enhanced Mobility and Comfort: Wheelchairs Empowered by SSVEP BCI for Instant Noise Cancellation and Signal Processing in Assistive Technology," *Electronics*, vol. 14, no. 21, 2025, doi: 10.3390/electronics14214338.

[44] Y. Wang, X. Chen, X. Gao, and S. Gao, "A Benchmark Dataset for SSVEP based Brain-Computer Interfaces," *IEEE Trans. Neural Syst. Rehabil. Eng.*, vol. 25, no. 10, pp. 1746-1752, Oct. 2017, doi: 10.1109/TNSRE.2016.2627556.

[45] M. Lee, H.-Y. Park, W. Park, K.-T. Kim, Y.-H. Kim, and J.-H. Jeong, "Multi-Task Heterogeneous Ensemble Learning-Based Cross-Subject EEG Classification Under Stroke Patients," *IEEE Trans. Neural Syst. Rehabil. Eng.*, vol. 32, pp. 1767-1778, 2024, doi: 10.1109/TNSRE.2024.3395133.

[46] Y. Cai, Q. She, J. Ji, Y. Ma, J. Zhang, and Y. Zhang, "Motor imagery EEG decoding using manifold embedded transfer learning," *J. Neurosci. Methods*, vol. 370, p. 109489, Mar. 2022, doi: 10.1016/j.jneumeth.2022.109489.

[47] J. Jiang, Z. Zhou, E. Yin, Y. Yu, and D. Hu, "Hybrid Brain-Computer Interface (BCI) based on the EEG and EOG signals," *Biomed. Mater. Eng.*, vol. 24, no. 6, pp. 2919-2925, Nov. 2014, doi: 10.3233/BME-141111.

[48] H. Wang, Y. Li, J. Long, T. Yu, and Z. Gu, "An asynchronous wheelchair control by hybrid EEG-EOG brain-computer interface," *Cogn. Neurodyn.*, vol. 8, no. 5, pp. 399-409, Oct. 2014, doi: 10.1007/s11571-014-9296-y.

[49] Q. Huang, Z. Zhang, T. Yu, S. He, and Y. Li, "An EEG/EOG-Based Hybrid Brain-Computer Interface: Application on Controlling an Integrated Wheelchair Robotic Arm System," *Front. Neurosci.*, vol. 13, Nov. 2019, doi: 10.3389/fnins.2019.01243.

AUTHOR BIOGRAPHY



Anderias Eko Wijaya earned his Bachelor's degree in Engineering from STMIK Subang in 2007 and completed his Master's degree in Computer Science at STMIK LIKMI Bandung in 2011. He is currently a lecturer in the Faculty of Engineering at Universitas Mandiri, where he teaches and supervises research in computer science and engineering. His primary research interests lie in Artificial Intelligence and the Internet of Things (IoT), encompassing various applications such as machine learning, deep learning, decision support systems, brain-computer interface (BCI), and drone optimization. In addition to academic teaching, he is also involved in applied research and technology development projects that integrate AI and IoT to address practical problems. His works contribute to advancing innovative systems, intelligent decision-making, and automation, particularly in robotics and BCI-based applications. Through his research and teaching, he is committed to fostering innovation and preparing future professionals with strong foundations in emerging technologies.



Nurizati received her Bachelor's degree in Physics from Institut Teknologi Bogor (IPB), Bogor, Indonesia, in 2007. Her undergraduate thesis was titled "Identification of Human Bone Mineral Composition with Variation of Age by Fourier Transform Infrared (FTIR)." She then pursued her Master's degree in Physics at the University of Indonesia, Depok, graduating in 2010. Her Master's thesis, "Monte Carlo Calculation Simulation of Fetal Dose in a Box-Shaped Breast Cancer Model with 2 MeV Photons. Since 2021, she has been a lecturer at the Department of Physics, Faculty of Science, Mandiri University, Subang, Indonesia. Her research interests lie primarily in medical physics and biomedical engineering.



Rian Hermawan received his Bachelor's degree in Engineering from STMIK Subang in 2016 and his Master's degree in Computer Science from STMIK LIKMI Bandung in 2018. He is currently a lecturer at Universitas Mandiri, Subang, Indonesia, focusing on teaching and research in computer science and applied technology. His primary research interests include the Internet of Things (IoT) and its applications in industrial and community-based innovation. He is actively involved in mentoring students and advancing

the development of sustainable IoT-based solutions for real world challenges.



Muhamad Agung Suhendra received his B.Sc. in Physics from UIN Sunan Gunung Djati, Bandung, Indonesia, in 2015, and his M.Sc. in Engineering Physics from Institut Teknologi Bandung, Bandung, Indonesia, in 2020. He has been serving as a lecturer in the Department of Physics, Faculty of Science, Universitas Mandiri, Subang, Indonesia, since 2021. In addition to his role as a lecturer, he currently serves as the Vice Dean for Academic Affairs at the Faculty of Science. His current research interests include cognitive science, biomedical signal processing, brain-computer interface (BCI), instrumentation, and control. In 2024, he received a research grant from Kemendikbudristekdikti through the Matching Fund program, in collaboration with PT Cakra Vimana DiinamyCx and BRIN. The project is titled "Robust Adaptive Mind Control for Aerial Robotic System".